Journal of Plant Physiology 175 (2015) 59–67

Contents lists available at ScienceDirect

Journal of Plant Physiology

journal homepage: www.elsevier.com/locate/jplph

Molecular Biology

The methylation status of plant genomic DNA influences PCR efficiency

K.V. Kiselev [1,2,*], A.S. Dubrovina [1], A.P. Tyunin [1]

[1] Laboratory of Biotechnology, Institute of Biology and Soil Science, Far East Branch of Russian Academy of Sciences, Vladivostok 690022, Russia
[2] Department of Biochemistry, Microbiology and Biotechnology, The School of Natural Sciences, Far Eastern Federal University, 690090, Vladivostok, Russia

ARTICLE INFO

Article history:
Received 14 May 2014
Received in revised form 11 October 2014
Accepted 12 October 2014
Available online 27 November 2014

Keywords:
Plant DNA extraction
Proteinase K
HotTaq DNA polymerase
Vitis amurensis
Arabidopsis thaliana

ABSTRACT

During the polymerase chain reaction (PCR), which is a versatile and widely used method, certain DNA sequences are rapidly amplified through thermocycling. Although there are numerous protocols of PCR optimization for different applications, little is known about the effect of DNA modifications, such as DNA methylation, on PCR efficiency. Recent studies show that cytosine methylation alters DNA mechanical properties and suggest that DNA methylation may directly or indirectly influence the effectiveness of DNA amplification during PCR. In the present study, using plant DNA, we found that highly methylated plant DNA genomic regions were amplified with lower efficiencies compared to that for the regions methylated at a lower level. The correlation was observed when amplifying stilbene synthase (*STS1*, *STS10*) genes of *Vitis amurensis*, the *Actin2* gene of *Arabidopsis thaliana*, the internal transcribed spacer (*AtITS*), and *tRNAPro* of *A. thaliana*. The level of DNA methylation within the analyzed DNA regions has been analyzed with bisulfite sequencing. The obtained data show that efficient PCRs of highly methylated plant DNA regions can be hampered. Proteinase K treatment of the plant DNA prior to PCR and using HotTaq DNA polymerase improved amplification of the highly methylated plant DNA regions. We suggest that increased DNA denaturation temperatures of the highly methylated DNA and contamination with DNA-binding proteins contribute to the hampered PCR amplification of highly methylated DNA. The data show that it is necessary to use current DNA purification protocols and commercial kits with caution to ensure appropriate PCR product yield and prevent bias toward unmethylated DNA amplification in PCRs.

Introduction

The polymerase chain reaction (PCR) is a versatile laboratory technique that is widely used in multiple fields, such as forensic medicine, diagnostics of various diseases, virology, bacteriology, or plant science. Success in using PCR depends on numerous conditions, such as template concentration and quality, design of primers, annealing temperature, buffer conditions, or polymerase type. Although there are numerous protocols of PCR optimization for different applications, little is known about the effect of DNA modifications, such as DNA methylation, on PCR efficiency.

A recent study revealed that cytosine methylation alters DNA mechanical properties (Severin et al., 2011). The authors found that there is a strong dependence of DNA strand separation on DNA methylation: DNA methylation was observed to either inhibit or facilitate strand separation, depending on methylation level and sequence context. It has been suggested that DNA methylation may regulate gene expression not only through mechanisms already known but also through changing mechanical properties of DNA (Severin et al., 2011). In the light of this investigation and some other studies, it is reasonable to propose that DNA methylation is likely to have an impact on DNA amplification in PCR. It already known that 5-methylcytosine increases the melting temperature (T_m) of DNA (Rand et al., 2006; Diede et al., 2010). Several techniques of DNA methylation analysis have been developed based on this property of methylated DNA (Rand et al., 2006; Diede et al., 2010). Furthermore, in a recent study, Bunyan et al. (2011) have shown that DNA methylation status can affect the denaturation rate prior to PCR and affect PCR efficiency for methylated and unmethylated regions of human DNA. The authors have found that only the non-methylated allele of human *MEST* gene has been amplified when using short initial DNA denaturation step (2 min) of the analyzed samples of human DNA. Only upon PCR protocol modification by using a longer DNA denaturation step (12 min), both the methylated and non-methylated alleles could have been identifiable (Bunyan et al., 2011). To the best of our knowledge, no other analyses of DNA methylation effect on DNA amplification during PCR are available in the literature.

* Corresponding author. Fax: +7 423 2310193.
E-mail address: kiselev@biosoil.ru (K.V. Kiselev).

http://dx.doi.org/10.1016/j.jplph.2014.10.017
0176-1617/

Cytosine DNA methylation is an epigenetic modification that is important for maintaining genome stability and regulating gene expression in higher plants and other organisms (Gehring and Henikoff, 2007; Zhang et al., 2010; Vanyushin and Ashapkin, 2011). Growing evidence suggests that DNA methylation is implicated in regulating gene expression across plant development and in response to environmental stress (Boyko and Kovalchuk, 2008; Zhang et al., 2010). DNA methylation is often associated with gene silencing and is well-known to silence transposable elements (Okamoto and Hirochika, 2001). Cytosine methylation of nuclear DNA is more extensive and involves a wider range of methylation sites in plants than in animals (Vanyushin and Ashapkin, 2011). For example, absolute quantification by mass spectrometry revealed 14% of cytosines methylated in plants (*Arabidopsis thaliana*), only 8% in *Mus musculus* and 0.03% in *Drosophila melanogaster* (Capuano et al., 2014). It is possible that DNA methylation has a higher impact on amplification of plant genomic DNA than on amplification of DNA from other organisms.

In the present study, we report on different PCR efficiencies for amplifying plant DNA regions with different levels of DNA methylation. When amplifying different DNA coding and noncoding sequences of *Vitis amurensis* and *A. thaliana* in PCRs, we encountered difficulties in amplifying highly methylated DNA regions. Highly methylated 3′ end of the grapevine stilbene synthase (*VaSTS10*) gene was amplified with low efficiency in PCR compared to its 5′ end or central part, which are methylated at a considerably lower level. The amplification of the *VaSTS1* gene, which is uniformly methylated at a lower level compared to *VaSTS10*, resulted in a higher PCR product yield for all parts of the gene. The amplification of *Actin2* and *tRNAPro* DNA of *A. thaliana*, which were highly methylated at early stages of *Arabidopsis* development, resulted in low amounts of PCR products for the seedling stage. The DNA regions of *A. thaliana*, which have been found to be unmethylated at later stages of *Arabidopsis* development, were efficiently amplified. We proposed that high levels of plant genomic DNA methylation can negatively influence PCR efficiency directly or indirectly. Application of proteinase K prior to PCRs and HotTaq DNA polymerase considerably improved amplification of the highly methylated DNA regions.

Materials and methods

Plant materials and growth conditions

The callus culture V2 was established in 2002 from the stems of wild-growing grapevine *Vitis amurensis* Rupr. (Vitaceae) (Kiselev et al., 2007). The V2 callus culture was cultivated with 35-day subculture intervals in the dark at 23–24 ± 1 °C in test tubes with 15 ml of Murashige and Skoog (MS) modified solid medium $W_{B/A}$ (Kiselev et al., 2012). MS medium was modified by decreasing NH_4NO_3 to 400 mg/l. This medium was supplemented with the following components (mg/l): thiamine HCl (0.2), nicotinic acid (0.5), pyridoxine HCl (0.5), meso-inositol (100), peptone (100), sucrose (25,000) and agar (6000) (denoted as W_0 medium). W_0 medium supplemented with 0.5 mg/l 6-benzylaminopurine (B) and 2 mg/l α-naphthaleneacetic acid (A) was designated as $W_{B/A}$. Sterile aqueous solutions of salicylic acid (SA) were added to the autoclaved media at the concentrations of 50 and 300 μM as described (Kiselev et al., 2010, 2013a). Plants of *A. thaliana* ecotype Columbia L., stored by our lab were grown in pots filled with commercially available rich soil in a controlled environmental chamber at +22 ± 1 °C (KS-200 SPU, Smolensk, Russia) kept on a 16/8 h day/night cycle at a light intensity of ~70 μmol m^{-2} s^{-1}.

DNA extraction

For the DNA purification, calli were harvested from 32 day cultures during their linear growth phase. For DNA purification, the V2 calli, untreated and treated with SA, were dried, ground in a mortar and thoroughly mixed. 20 mg of the obtained powder of the V2 cell culture was used for DNA isolation. We used different stages of *A. thaliana* life cycle: two *A. thaliana* plants were collected every 1, 4, 8, and 12 weeks after seed sowing. The 1-week-old seedlings of *A. thaliana* were used for DNA purification without drying (1 seedling per purification). The 4-, 8-, and 12-week-old plants of *A. thaliana* were dried, ground in a mortar and thoroughly mixed for the following DNA purification. 10 mg of the obtained powder of *A. thaliana* plants was used for DNA isolation.

Total DNA was extracted as described previously (Echt et al., 1992) with some modifications. The plant tissue was mixed with 800 μl of the homogenization buffer containing 0.2% mercaptoethanol, 100 mM Tris (pH 7.5–8.0), 0.7 M NaCl, 40 mM EDTA (pH 7.5–8.0), and 1% cetyltrimethylammonium bromide (CTAB). The mixture was incubated at +60 °C for 1 h under stirring. Then, the samples were vigorously mixed with 300 μl of chloroform during 5 min and centrifuged at 13–14,000 rpm for 5 min. 300–400 μl of the aqueous phase were precipitated with 2.5 V 96% ethanol (at −20 °C for 20 min) and pelleted by spinning in a microcentrifuge at 13–14,000 rpm for 5 min. The DNA samples were dried at +37 °C and dissolved in 100–500 μl of distilled water depending of the pellet size. Total DNA concentration was measured with a spectrophotometer (RF-1501, Shimadzu, Japan). We used DNA with the ratio of the absorbance at 260 and 280 nm ($A_{260/280}$) higher than 1.8. For PCRs, we used 0.05–0.1 μg of the total DNA.

After DNA isolation, we treated the purified DNA with proteinase K prior to PCRs in some cases. 18 μl of the extracted DNA was mixed with 2 μl of the proteinase K solution (12.5 μg/ml) in W buffer: 10 mM Tris–HCl, pH 8.5 in 25 °C; 10 mM $MgCl_2$; 100 mM NaCl; 1 mM DTT (SibEnzyme, Novosibirsk, Russia). The mixture was incubated at +50 °C for 15 min in thermostat Gnom (DNA technology, Moscow, Russia). Then, the samples were gently mixed with 50 μl of 96% ethanol, incubated at −20 °C for 30 min, and centrifuged at 13–14,000 rpm for 15 min. The DNA samples were dried at +37 °C and dissolved in 15 μl of distilled water.

PCR analysis

Amplification reactions were performed in volumes of 20 μl containing 70 mM Tris–HCl (pH 8.6), 17 mM $(NH_4)_2SO_4$, 2.5 mM $MgCl_2$, 0.2 mM of each dNTP, 0.2 μM of each oligonucleotide primer and 2 units of DNA polymerase (a mix 1:6 of Pfu and Taq polymerases "Silex M", Moscow, Russia). Analysis was performed in a T100 Thermal Cycler (Bio Bio-Rad Laboratories, Inc., Hercules, CA, USA) programmed for an initial denaturation step of 2 min at 95 °C followed by 28–40 cycles of 15 s at 95 °C, 10 s at 52–54 °C, 25–42 s at 72 °C, and 2 min at 72 °C. For some PCR reactions we used 2 units of HotTaq polymerase ("Silex M", Russia) with the first denaturation step being 10 min at 95 °C and the buffer containing 70 mM Tris–HCl (pH 8.3), 17 mM $(NH_4)_2SO_4$, 2.5 mM $MgCl_2$. The gene-specific primer pairs are presented in Table S1.

Amplification of V. amurensis genomic DNA regions. We divided *VaSTS1* (GenBank acc. no GQ167204) and *VaSTS10* (GenBank acc. no JQ780328) gene sequences into three parts and designed specific primers to amplify each fragment (Fig. 1). The primers *STS1*-C1 S1 and A1 were designed based on the beginning of the *VaSTS1* gene and were used for amplification of a 689-bp fragment of the *STS1* gene (GC content 44.4%), annealing temperature (T_a) 54 °C, elongation time 35 s. The primers *STS1*-C2 S2 and A2 were designed based on the central part of the *VaSTS1* gene and were used for

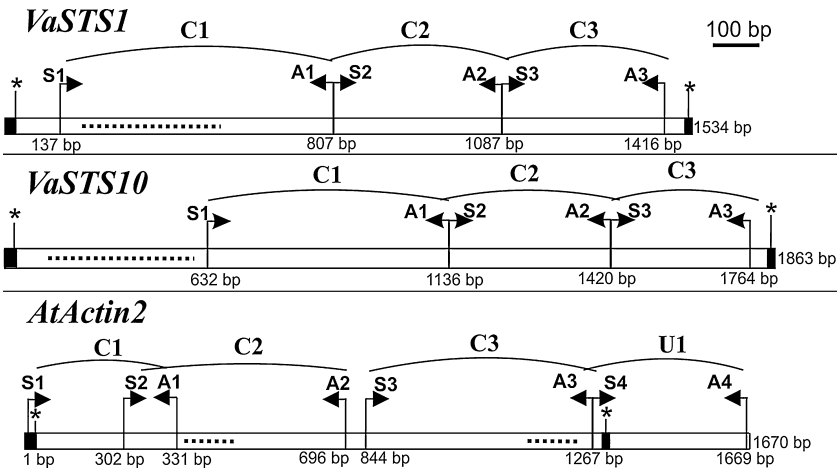

Fig. 1. Schematic presentation of the *VaSTS1*, *VaSTS10*, and *AtActin2* gene sequences with the positions of the specific primers used in PCR analysis. Asterisks depict positions of the start and stop codons. Dashed lines depict positions of the introns. C1, C2, C3, U1 – DNA regions used for DNA amplification. S1–S4, A1–A4 – sense and antisense primers used for DNA amplification.

amplification of a 303-bp fragment of the *STS1* gene (GC content 46.5%), T_a 54 °C, elongation time 25 s. The primers *STS1*-C3 S3 and A3 were designed based on the end of the coding region the *VaSTS1* gene and were used for amplification of a 348-bp fragment of the *STS1* gene (GC content 43.1%), T_a 54 °C, elongation time 25 s. The primers *STS10*-C1 S1 and A1 were designed based on the beginning of the *VaSTS10* gene and were used for amplification of a 523-bp product of the *STS10* gene (GC content 45.9%), T_a 54 °C, elongation time 30 s. The primers *STS10*-C2 S2 and A2 were designed based on the central part of the *VaSTS10* gene and were used for amplification of a 303-bp product of the *STS10* gene (GC content 49.5%), T_a 54 °C, elongation time 25 s. The primers *STS10*-C3 S3 and A3 were designed based on the end of the coding region of the *VaSTS10* gene and were used for amplification of a 344-bp product of the *STS10* gene (GC content 40.1%), T_a 54 °C, elongation time 25 s. The identity of the PCR products of the amplified DNA regions of *V. amurensis* and *A. thaliana* was confirmed by DNA sequencing.

Amplification of A. thaliana genomic DNA regions. We divided *AtActin2* (GenBank acc. no NM_112764) gene sequences into four different fragments and designed specific primers to amplify each fragment (Fig. 1). The primers *Actin2*-C1 S1 and A1 were designed based on the beginning of the *AtActin2* gene coding sequence and were used for amplification of a 351-bp product of the *AtActin2* gene (GC content 46.4%), T_a 54 °C, elongation time 25 s. The primers *Actin2*-C2 S2 and A2 were designed based on the beginning of *AtActin2* coding sequence and were used for amplification of a 413-bp product of the *AtActin2* gene (GC content 45.3%), T_a 51 °C, elongation time 30 s. The primers *Actin2*-C3 S3 and A3 were designed based on the end of the coding region of the *AtActin2* gene coding sequence and were used for amplification of a 442-bp product of the *Actin2* gene (GC content 44.6%), T_a 52 °C, elongation time 30 s. The primers *Actin2*-U1 S4 and A4 were designed based on the 3′ UTR of the *AtActin2* gene (U1 region) and were used for amplification of a 401-bp product of the *AtActin2* gene (31 bp of the 3′ coding region and 370 bp of the 3′ UTR; GC content 32.6%), T_a 53 °C, elongation time 25 s. PCR was also used for amplification of partial sequences of *A. thaliana* internal transcribed spacer sequence *ITS1* and *ITS2* of ribosomal DNA with 5.8 S rRNA sequence between them. The primers *AtITS* S1 and A1 were designed based on the *A. thaliana ITS1*; 5.8S rRNA; *ITS2* sequence (GenBank acc. no X52320) and were used for amplification of a 728-bp product (*AtITS* region) from the ribosomal DNA region (GC content 54.9%), T_a 53 °C, elongation time 42 s. The primers *AttRNA* S1 and A1 were designed based on the nuclear *tRNA* sequence (GenBank acc. no CP002685 3,494,992–3,495,569 bp) and were used for amplification of a 576-bp product (*At-tRNAPro* region) from the nuclear DNA encoding for *tRNAPro* and some non-coding DNA sequence, T_a 54 °C, elongation time 33 s. The identity of the PCR products of the amplified DNA regions of *V. amurensis* and *A. thaliana* was confirmed by DNA sequencing. The gene-specific primer pairs are presented in Table S1.

The primer efficiency was tested using real-time PCR. To test the efficiency of primers designed to *VaSTS1* and *VaSTS10* genes, we used DNA of the V2 callus culture of *V. amurensis* cultivated in standard conditions. To test the efficiency of primers designed to the *A. thaliana* coding (*AtActin2*, *At-tRNAPro*) and noncoding (*AtITS*) DNA regions, DNA of *A. thaliana* was purified from the 12-week-old plants. The DNA of *V. amurensis* and *A. thaliana* (several dilutions) was amplified using EvaGreen Real-time PCR (Biotium, Hayward, USA) as described (Dubrovina et al., 2013).

Bisulfite sequencing

The cytosine methylation status of the *VaSTS1*, *VaSTS10*, *AtActin2*, *AtITS*, and *At-tRNAPro* DNA regions of *V. amurensis* and *A. thaliana* was analyzed using bisulfite sequencing as described (Kiselev et al., 2013b; Tyunin et al., 2013; Kiselev et al., 2014). For the DNA methylation analysis, we divided the *VaSTS1*, *VaSTS10*, and *AtActin2* gene sequences into several parts and designed specific primers to amplify each fragment (Fig. 2). The MC1, MC2, MC3, and MC4 coding regions of the *VaSTS1* and *VaSTS10* genes were amplified using the primer pairs shown in Table S1 and Fig. 2. The primers *AtActin2*-U1 S1 and A1 were used for amplification of a 361-bp fragment of the U1 region of the *AtActin2* 3′ UTR (Table S1; Fig. 2). The primers *At-tRNAPro* S1 and A1 were used for amplification of a 301-bp fragment of the *At-tRNAPro* DNA region (Table S1; Fig. 2). Notably, these primers used in bisulfite sequencing for the *Actin2*, *ITS*, and *tRNAPro* DNA of *A. thaliana* were designed to amplify DNA within the same *Actin2*, *ITS*, and *At-tRNAPro* regions used for analysis of PCR effectiveness. We used universal PCR program for all mentioned PCR primers for the converted DNA: an initial denaturation step of 2 min at 95 °C, followed by 40 cycles of 15 s at 95 °C, 15 s at 52 °C, 30 s at 72 °C, and a last cycle of 72 °C for 5 min, using the fastest available transitions between each temperature. The PCR products were isolated from agarose gels using a Cleanup Mini Kit (Eurogene, Moscow, Russia) and subcloned as described (Dubrovina et al., 2013; Kiselev et al., 2013a). The clones were amplified and sequenced using an ABI 3130

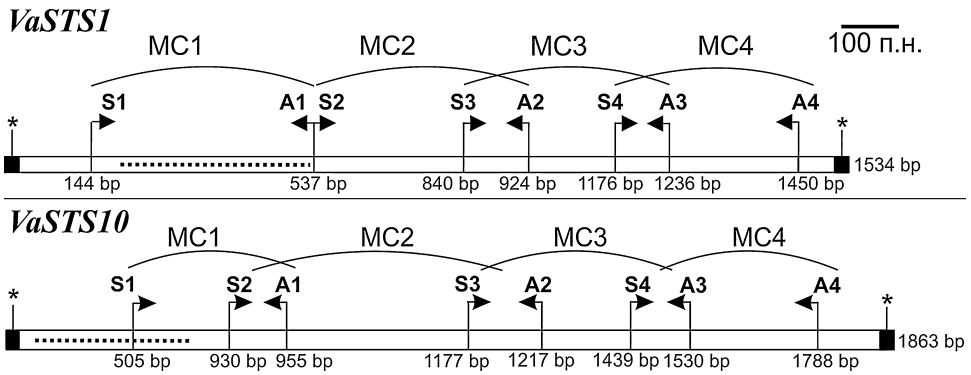

Fig. 2. Schematic presentation of the *VaSTS1* and *VaSTS10* fragments with the positions of the specific primers used in bisulfite sequencing. Asterisks depict positions of the start and stop codons. Dashed lines depict positions of the introns. MC1, MC2, MC3, MC4 – DNA regions used for bisulfite sequencing. S1–S4, A1–A4 – sense and antisense primers used for bisulfite sequencing.

Genetic Analyzer (Applied Biosystems, Foster City, CA, USA) following the manufacturer's protocol and recommendations as described (Kiselev et al., 2011). A total of 14 individual clones were sequenced for each region of the analyzed DNA regions (7 clones from two different plants). The Basic Local Alignment Search Tool (BLAST) program was used for sequence analysis. Multiple sequence alignments were performed using the ClustalX program (Altschul et al., 1990).

Statistical analysis

The statistical analysis was carried out using the Statistica 10.0 program (StatSoft Inc., Boston, USA). The data are presented as mean ± standard error (SEM) and were tested by paired Student's *t*-test. The 0.05 level was selected as the point of minimal statistical significance in all analyses.

Results and discussion

The effect of DNA methylation on VaSTS1 and VaSTS10 amplification

For the PCR analyses, the coding regions of the *VaSTS1* and *VaSTS10* genes were divided into C1, C2, and C3 parts of ~300–700 bp (Fig. 1) and individually PCR-amplified using the DNA purified from the callus cell culture V2 of *V. amurensis* cultivated in standard conditions and in the presence of 50 and 300 μM of salicylic acid (SA) (Fig. S1a and b). We noted that amplification of the 3′ end of the *VaSTS10* coding gene sequence (C3 region) resulted in a considerably lower yield of PCR product than amplification of its beginning (C1) or central parts (C2); however, amplification of the C1, C2, and C3 parts of the *VaSTS1* coding gene sequence resulted in a high PCR product yield in all PCR reactions (Figs. 1, S1a and b). For this purpose, we used DNA purified from the V2 cell culture cultivated in standard conditions and in the presence of salicylic acid (SA), because it has been shown that treatment with SA induced a significant decrease in cytosine methylation within the *VaSTS10* but not *VaSTS1* genes (Kiselev et al., 2014). Notably, amplification of the DNA purified from the V2 cell culture treated with 300 μM of SA resulted in larger amounts of *VaSTS10* PCR products compared to that from the untreated V2 cells (Fig. S1).

One can propose that the PCRs presented are at saturation, and thus the data is not quantitative. In order to study whether particular DNA regions are consistently amplified less well than other regions, we showed the PCR product amounts at different cycles of PCR (40, 36, 32, 28) by electrophoretic separation and quantification by densitometry of the PCR products of the analyzed *VaSTS1* and *VaSTS10* DNA regions (Fig. 3). The data show that the *VaSTS10* C3 gene region amplifies consistently less well than the C1 and C2 regions of *VaSTS10* (Fig. 3). We also noted that all analyzed regions of *VaSTS10* gene were amplified with a consistent lower effectiveness than that of *VaSTS1* (Fig. 3). Fig. S1, we presented PCR products after 40 cycles of amplification, since the difference in PCR product yield for the C1, C2 and C3 regions was the most evident. Similar results were obtained after 36, 32 and 28 PCR cycles of amplification.

Notably, the primers designed to amplify the *VaSTS10* gene were efficient at approximately the same level compared with the primers for *VaSTS1*. We compared efficiency of all used primer pairs in the present study using real-time PCR and the same template (several serial dilutions) for all the primer pairs for *V. amurensis*, including the primers for *VaSTS1* and *VaSTS10*, and the same template for all primer pairs for *A. thaliana*. The efficiency of all primer pairs was high (97–115%) and did not considerably differ, including primers for *VaSTS10* (Table S2).

Since it has been previously shown that the *VaSTS1* and *VaSTS10* genes are differentially methylated in the DNA purified from VV cell culture of *V. amurensis* (Kiselev et al., 2013b; Tyunin et al., 2013), and SA induced a considerable decrease in the cytosine methylation level (Kiselev et al., 2014), we proposed that a high DNA methylation level could negatively affect amplification of the *VaSTS10* 3′-coding end and amplification of the *VaSTS10* in general compared to *VaSTS1*, when we amplified DNA of the V2 cell culture. In the present study, we analyzed DNA methylation levels of the *VaSTS1* and *VaSTS10* genes in the DNA of the used V2 callus cell culture of *V. amurensis*, which is the parent cell line for the VV cell culture, using bisulfite sequencing (Fig. 4 and Table 1). For the DNA methylation analysis, we used DNA purified from the V2 cell culture cultivated in standard conditions. Due to bisulfite

Table 1
Methylation status of the CHH, CG, and CHG sites in the MC1, MC2, MC3, and MC4 regions of the *VaSTS1* and *VaSTS10* genes in the DNA of the V2 callus culture of *Vitis amurensis* cultivated under normal conditions.

	DNA region	CHH	CG	CHG
VaSTS1	MC1	17.1 ± 1.2	15.6 ± 1.1	22.6 ± 1.4
	MC2	19.3 ± 2.2	16.7 ± 2.2	23.8 ± 1.2
	MC3	18.2 ± 1.9	16.2 ± 1.2	23.1 ± 1.3
	MC4	16.2 ± 1.7	24.6 ± 2.5	30.3 ± 2.7
VaSTS10	MC1	34.1 ± 2.3**	39.2 ± 4.1**	36.9 ± 2.6*
	MC2	29.3 ± 2.1*	33.1 ± 2.3**	30.3 ± 2.8*
	MC3	34.5 ± 2.5**	38.9 ± 2.5**	37.2 ± 2.4*
	MC4	55.4 ± 3.7**	55.1 ± 4.4**	69.0 ± 5.1**

* $P < 0.05$ when compared to the values of the methylation status of *VaSTS1* gene and appropriate methylation site.
** $P < 0.01$ when compared to the values of the methylation status of *VaSTS1* gene and appropriate methylation site.

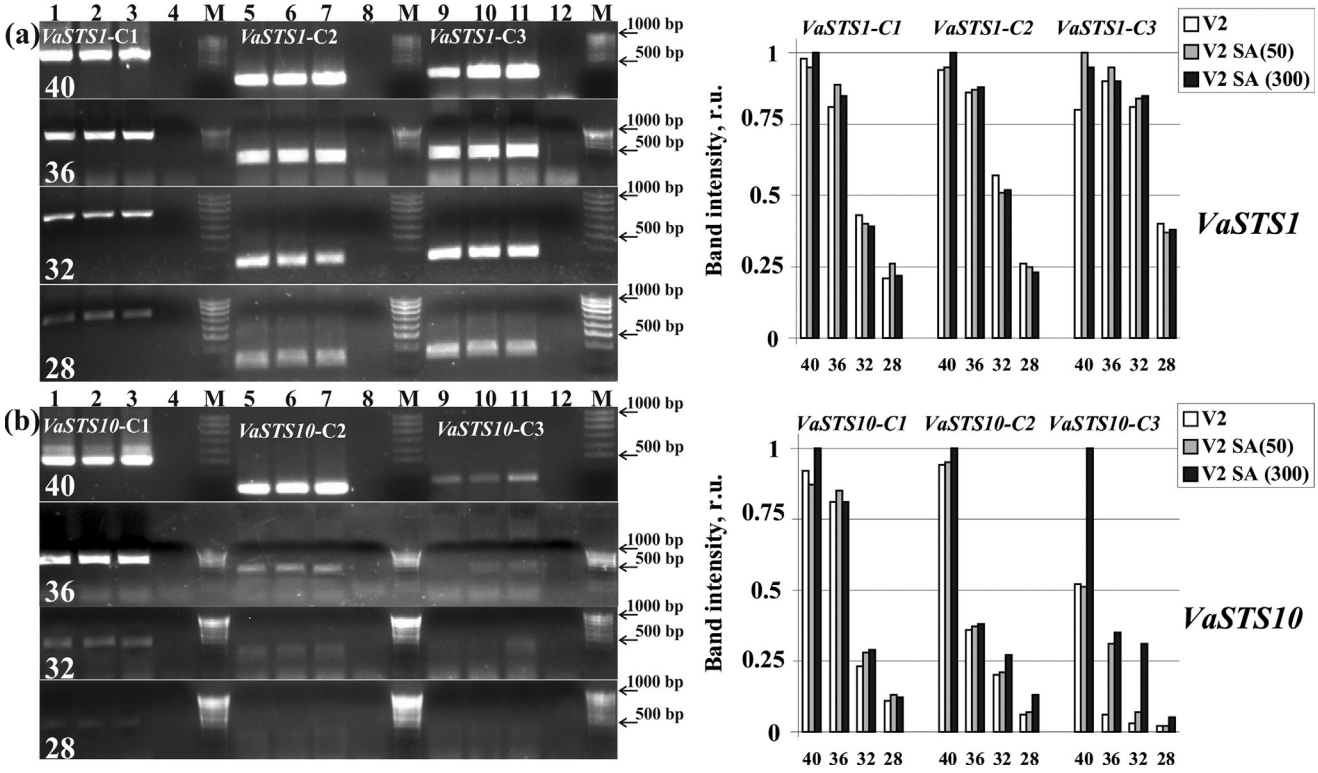

Fig. 3. Electrophoretic separation and quantification by densitometry of PCR products of the *VaSTS1* (*VaSTS1*-C1, C2, and C3) and *VaSTS10* (*VaSTS10*-C1, C2, and C3) DNA regions of *Vitis amurensis* after 40, 36, 32, and 28 cycles. DNA was extracted from the V2 cell culture of *V. amurensis* cultivated in normal conditions (lanes 1, 5, 9) and after treatment with SA at a concentration of 50 μM (lanes 2, 6, 10) and 300 μM (lanes 3, 7, 11). Lanes 4, 8, 12: negative control (PCR mixture without plant DNA); lane M: synthetic marker.

sequencing technique limitations, we divided the *VaSTS1* and *VaSTS10* genes sequences into four fragments of ~400 bp: MC1 – beginning; MC2, MC3 – central part; and MC4 – end of the *STS* genes coding region (Fig. 2). These fragments were analyzed individually using bisulfite sequencing to determine the cytosine methylation levels (Fig. 4). We found that, in standard cultivation conditions, the 3′ end of the *VaSTS10* gene was methylated at a significantly higher level than its beginning or central parts (Fig. 4 and Table 1). At the same time, the level of *VaSTS1* methylation did not considerably vary over its coding sequence (Fig. 4 and Table 1). The degree of *VaSTS1* methylation was significantly lower than the degree of *VaSTS10* methylation (Fig. 4). The data are consistent with the data on *VaSTS1* and *VaSTS10* methylation in the VV cell culture (Kiselev et al., 2013b; Tyunin et al., 2013).

Thus, a correlation between the PCR product yield and the level of DNA methylation of the amplified DNA regions was observed for the *STS1* and *STS10* genes of *V. amurensis* (Figs. 3, 4 and S1). The highly methylated 3′ end of the *VaSTS10* coding region was

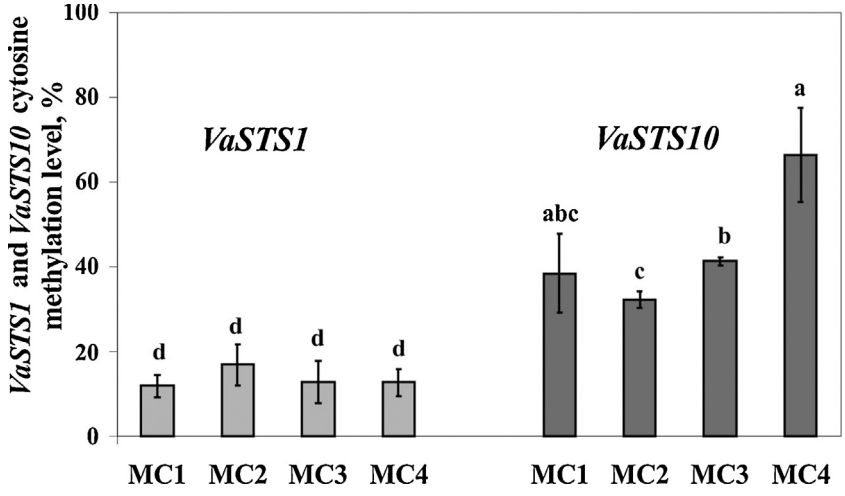

Fig. 4. Analysis of the total DNA methylation status within the different protein coding regions of the *VaSTS1* and *VaSTS10* genes in the V2 callus culture of *V. amurensis* cultivated under normal conditions. MC1: methylation levels within the MC1 region of *VaSTS1* and *VaSTS10* coding sequences; MC2: methylation levels within the MC2 region of *VaSTS1* and *VaSTS10* coding sequences; MC3: methylation levels within the MC3 region of *VaSTS1* and *VaSTS10* coding sequences; MC4: methylation levels within the MC4 region of *VaSTS1* and *VaSTS10* coding sequences. Mean ± SE followed by the same letter were not different using Student's *t*-test. $p < 0.05$ was considered to be statistically significant.

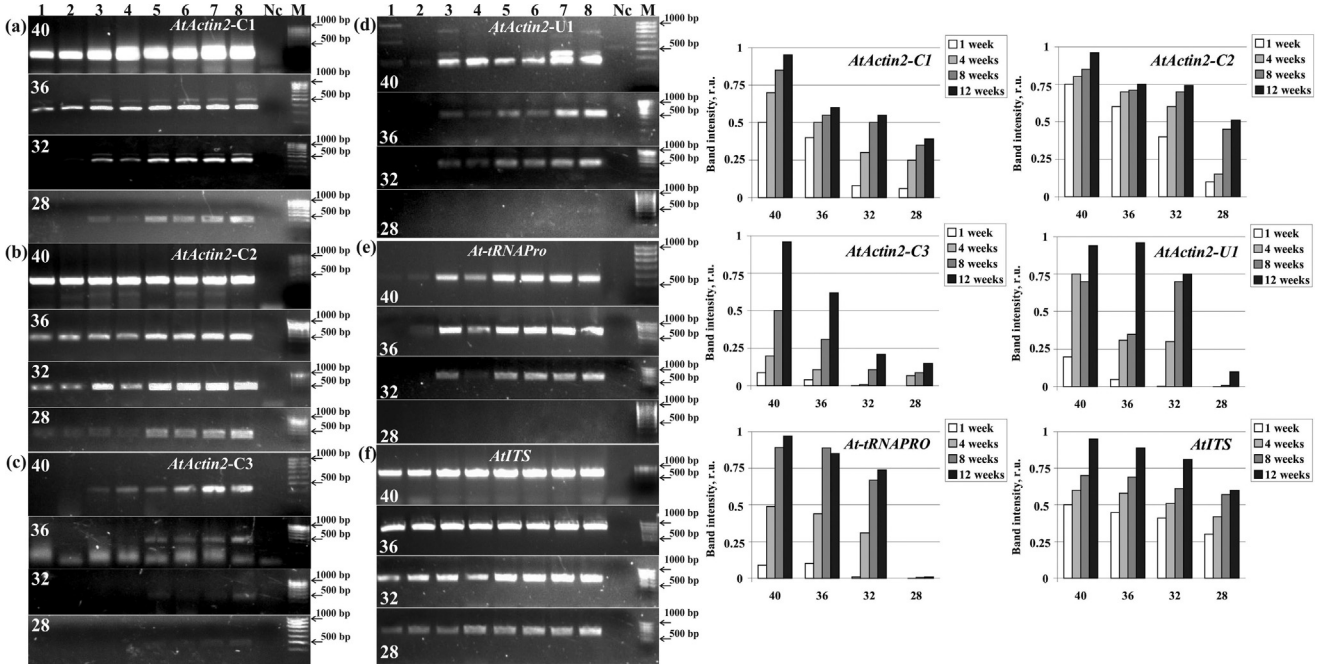

Fig. 5. Electrophoretic separation and quantification by densitometry of PCR products of the *AtActin2*, *AtITS*, and *At-tRNAPro* DNA regions of *Arabidopsis thaliana* after 40, 36, 32, and 28 cycles. DNA was extracted from the plants collected at different stages of the *Arabidopsis* life cycle. Two *A. thaliana* plants were collected every 1 (lanes 1 and 2), 4 (lanes 3 and 4), 8 (lanes 5 and 6), and 12 (lanes 7 and 8) weeks after seed sowing. *AtActin2*-C1 – primers were selected for the beginning of the *AtActin2* coding sequence (a); *AtActin2*-C2 – primers were selected for the central part of the *AtActin2* coding sequence (b); *AtActin2*-C3 – primers were selected for the end of the *AtActin2* coding sequence (c); *AtActin2*-U1 – primers were selected for 3′ UTR region of the *AtActin2* gene (d); *At-tRNAPro* – primers were selected for the *tRNAPro* DNA of *A. thaliana* (e); *AtITS* – primers were selected for the *ITS1-5.8S rRNA-ITS2* DNA of *A. thaliana* (f); lane Nc: negative control (PCR mixture without plant DNA); lane M: synthetic marker.

amplified with a low efficiency compared to other *VaSTS10* regions, which were less methylated. The obtained data suggest that DNA methylation directly or indirectly hampered amplification of the *VaSTS10*-C3 DNA region.

We analyzed the methylation status at the CHH, CG, and CHG sites of the *VaSTS1* and *VaSTS10* MC1, MC2, MC3, and MC4 regions in the DNA of the V2 callus culture of *V. amurensis* cultivated under standard conditions (Table 1). In general, all analyzed DNA regions of the *VaSTS10* gene were methylated at higher levels within the CHH, CG, and CHG sites compared with the methylation level within the sites of the *VaSTS1* gene. We noted that the methylation level within the CHH, CG, and CHG sites of the MC4 region of the *VaSTS10* gene was higher than in the MC1, MC2, MC3 regions and exceeded 55% (Table 1). It is possible that all parts of the *VaSTS10* gene were more difficult to amplify in PCRs than that of *VaSTS1* because of the high methylation level and high methylation level within CHH sites (Table 1 and Fig. 3).

The effect of Arabidopsis DNA methylation on PCR product yield

In our earlier research work, we noted that amplification of some DNA regions of *A. thaliana* was not efficient, despite optimization of PCR conditions. In the present work, we discovered that there is a correlation between the cytosine methylation level and the effectiveness of DNA amplification of these coding and noncoding DNA regions of *A. thaliana*. Several coding and noncoding DNA regions of *A. thaliana*, namely *Actin2* gene sequence (*AtActin2*), the internal transcribed spacer sequence *ITS1-5.8 rRNA-ITS2* (*AtITS*), and the nuclear *tRNAPro* coding DNA (*At-tRNAPro*), have been analyzed. In order to assess PCR efficiency, we divided the *AtActin2* sequence into four fragments of ~351–442 bp: C1 – beginning; C2 – central part, and C3 – the end of the *AtActin2* coding region; U1 – 3′ UTR of *AtActin2* (Fig. 1).

For the following PCRs (Fig. S2a–d), DNA has been purified from *A. thaliana* plants at different stages of the *Arabidopsis* life cycle. We collected the above-ground vegetative *A. thaliana* tissues 1 week post-sowing (seedlings with two cotyledons), 4 weeks post-sowing (full rosette with emerging flower shoots), 8 weeks post-sowing (full rosette with developed flower shoots and developing siliques), and 12 weeks post-sowing (seed maturation and plant senescence). The yield of *AtActin2* PCR products was high and approximately identical for the beginning (C1) and central (C2) parts of the *AtActin2* gene (Fig. S2a and b), while it dramatically decreased for the 3′ end (C3) and 3′ UTR (U1) of the *AtActin2* (Fig. S2c and d), especially for the seedling stage. Similarly to amplification of the *AtActin2*, amplification of the nuclear *At-tRNAPro* sequence revealed that PCR product yield was also considerably lower for 1-week-old *A. thaliana* seedlings than that for later stages of *A. thaliana* development (Fig. S2e). However, there were no so substantial differences in PCR products yield of *AtITS* for the *A. thaliana* plants of different ages (Fig. S2f). In order to study whether particular DNA regions of *A. thaliana* are consistently amplified less well than other regions, we showed the PCR product amounts at different cycles of PCR (40, 36, 32, 28) by electrophoretic separation and quantification by densitometry of the PCR products (Fig. 5). The data show that the *AtActin2*-C3, *AtActin2*-U1, and *tRNAPro* DNA regions of *A. thaliana* are amplified consistently less well than *AtActin2*-C1, *AtActin2*-C2, and *AtITS* DNA regions (Fig. 5). This was especially evident for the DNA of *A. thaliana* purified from 1-week-old *A. thaliana* seedlings (Fig. 5). For example, the *AtActin2*-C3, *AtActin2*-U1, and *tRNAPro* PCR products were hardly visible after 40 PCR cycles of amplification of the DNA purified from the *A. thaliana* seedlings, while high amounts of PCR products were visible for other DNA regions and for other stages of *Arabidopsis* development (Fig. 5).

The cytosine methylation levels were analyzed within the *AtActin2-U1*, the *AtITS* and *At-tRNAPro* regions of *A. thaliana* DNA using bisulfite sequencing of the DNA extracted from the different stages of *A. thaliana* life cycle (Fig. 6). The data show that the level of cytosine methylation within the 3′ UTR *AtActin2* (U1) and the *At-tRNAPro* DNA regions gradually decreased during plant

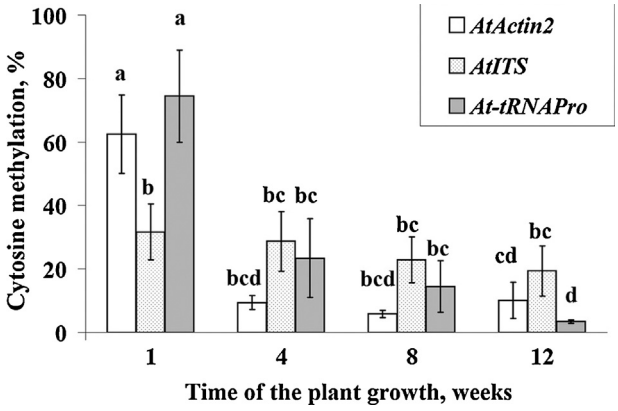

Fig. 6. Analysis of the total DNA methylation status within the *AtActin2* gene 3′ UTR (U1), the *At-tRNAPro*, and the *AtITS* DNA regions. Mean ± SE followed by the same letter were not different using Student's *t*-test. $p < 0.05$ was considered to be statistically significant.

development and maturation from 63% and 75% in 1-week-old *A. thaliana* seedling to 10% and 3% in 12-week-old *A. thaliana* plants, respectively (Fig. 6). DNA methylation analysis indicated that the level of DNA methylation within the *AtITS* sequence did not considerably vary throughout the *Arabidopsis* life cycle (Fig. 6). Notably, the total level of *AtITS* methylation was considerably lower than the total level of *AtActin2* and *At-tRNAPro* methylation at the seedling stage (Figs. S2e, f and 6). The lower level of *AtITS* methylation correlated with a higher efficiency of its DNA amplification (Figs. 5, 6 and S2). Thus, the obtained data show that highly methylated DNA regions of *A. thaliana* are amplified with a low effectiveness in PCR, while less methylated regions are efficiently amplified, and this suggests that high levels of DNA methylation directly or indirectly hamper effective DNA amplification.

We analyzed the methylation status at the CHH, CG, and CHG sites of the *AtActin2-U1*, *AtITS*, and *tRNAPro* regions in the DNA extracted from the *A. thaliana* plants collected every 1, 4, 8, and 12 weeks after seed sowing (Table 2). The high methylation levels of *AtActin2-U1* and *At-tRNAPro* at the CHH, CG, and CHG sites were similar and gradually decreased during plant growth (in 12.6–49.2 times). The methylation level of *AtITS* at the CG and CHG sites was in 1.6–3.9 times higher compared with that at the CHH sites. During *Arabidopsis* growth, the CG and CHG methylation of *AtITS*

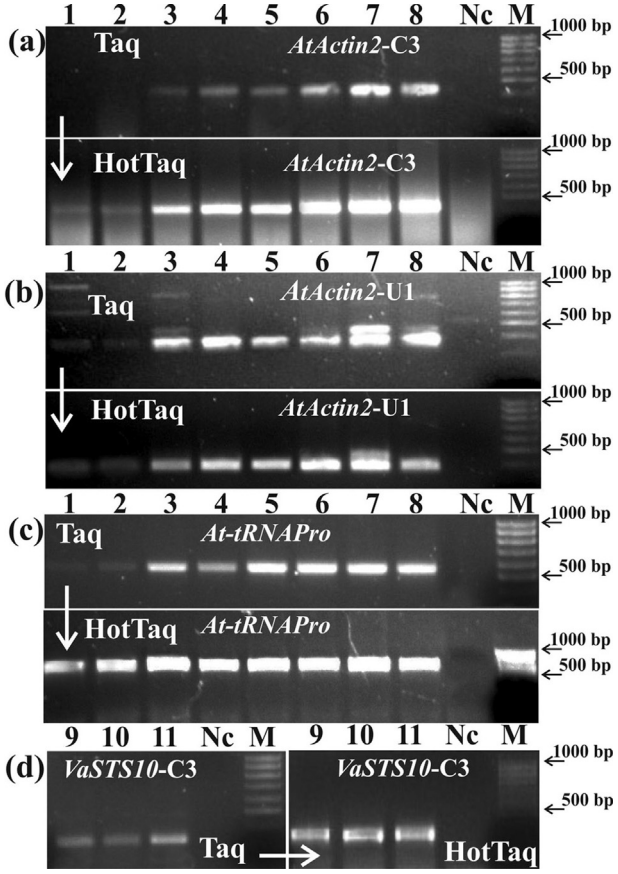

Fig. 7. Electrophoretic separation of PCR products of the *Actin2* gene of *A. thaliana* (a and b), *At-tRNAPro* DNA of *A. thaliana* (c) and *VaSTS10* gene of *V. amurensis* (d) obtained using either Taq or HotTaq polymerases after 40 PCR cycles. DNA was extracted from the plants collected at different stages of *A. thaliana* life cycle. Two *A. thaliana* plants were collected every 1 (lanes 1 and 2), 4 (lanes 3 and 4), 8 (lanes 5 and 6), and 12 (lanes 7 and 8) weeks after seed sowing. The DNA was extracted from the V2 callus culture of *V. amurensis* cultivated in normal conditions (lane 9) and after treatment with SA at a concentration of 50 μM (lane 10) and 300 μM (lane 11). *AtActin2*-C3 – primers were selected for the end of the *AtActin2* coding sequence (a); *AtActin2*-U1 – primers were selected for 3′ UTR region of the *AtActin2* gene (b); *At-tRNAPro* – primers were selected for the *At-tRNAPro* DNA of *A. thaliana* (c); *VaSTS10*-C3 – primers were selected for the end of *VaSTS10* coding region (d). Lane Nc: negative control (PCR mixture without plant DNA); lane M: synthetic marker.

Table 2
Methylation status of the CHH, CG, and CHG sites in the *AtActin2-U1*, *AtITS*, *At-tRNAPro* regions in the DNA extracted from the *Arabidopsis thaliana* plants collected every 1, 4, 8, and 12 weeks after seed sowing.

	Time (weeks)	CHH	CG	CHG
AtActin2-U1	1	60.3 ± 0.7	61.8 ± 1.3	62.1 ± 1.4
	4	5.9 ± 1.4**	0**	0**
	8	3.6 ± 1.4**	0**	0**
	12	4.8 ± 1.3**	2.4 ± 1.7**	4.6 ± 2.5**
AtITS	1	15.6 ± 3.1	51.6 ± 3.4	46.2 ± 7.2
	4	14.7 ± 2.4	46.7 ± 1.6	27.4 ± 2.2*
	8	10.9 ± 1.2	42.7 ± 1.5*	25.3 ± 1.7*
	12	11.7 ± 2.6	25.4 ± 3.8**	18.5 ± 8.1*
At-tRNAPro	1	72.5 ± 3.7	73.8 ± 5.3	75.1 ± 6.2
	4	36.3 ± 2.5*	34.2 ± 1.5*	34.4 ± 1.9*
	8	18.7 ± 1.2**	20.1 ± 2.2**	19.6 ± 1.6**
	12	3.4 ± 2.1**	1.5 ± 0.8**	3.2 ± 1.8**

* $P < 0.05$ when compared to the values of the selected DNA region for the 1-week-old seedlings of *A. thaliana* for each methylation site.
** $P < 0.01$ when compared to the values of the selected DNA region for the 1-week-old seedlings of *A. thaliana* for each methylation site.

significantly decreased. At the same time, the methylation level of *AtITS* at the CHH position decreased only slightly during plant growth, and this decrease was not statistically significant (Table 2). Obviously, the occurrence of CHH sites in the DNA is generally higher than that of CG and CHG sites. Probably, low level of methylation at the CHH sites in all used plant stages of *A. thaliana* was an indirect or direct reason for the higher PCR efficiency of the analyzed DNA regions of *A. thaliana*.

Using primers for *VaSTS10* (*STS10*-C1 S1 and *STS10*-C3 A3) and for *AtActin2* (*Actin2*-C1 S1 and *Actin2*-U1 A4) on the total DNA, we obtained PCR products of the full-length *VaSTS10* and *AtActin2* genes. Then, we diluted the PCR products (1:10) and used these dilutions in new PCRs with the necessary primers for different fragments of the *VaSTS10* and *AtActin2* genes (Fig. S3). We used 28, 32, 36, and 40 cycles in the PCR reactions and we detected high PCR product yields in all probes (Fig. S3). Therefore, all used primers for *VaSTS10* and *AtActin2* amplification possess high efficiency. The data confirm that DNA methylation directly or indirectly hampered amplification of the *VaSTS10*-C3, *AtActin2*-C3, and *AtActin2*-U1 regions when using DNA isolated from *V. amurensis* and *A. thaliana*.

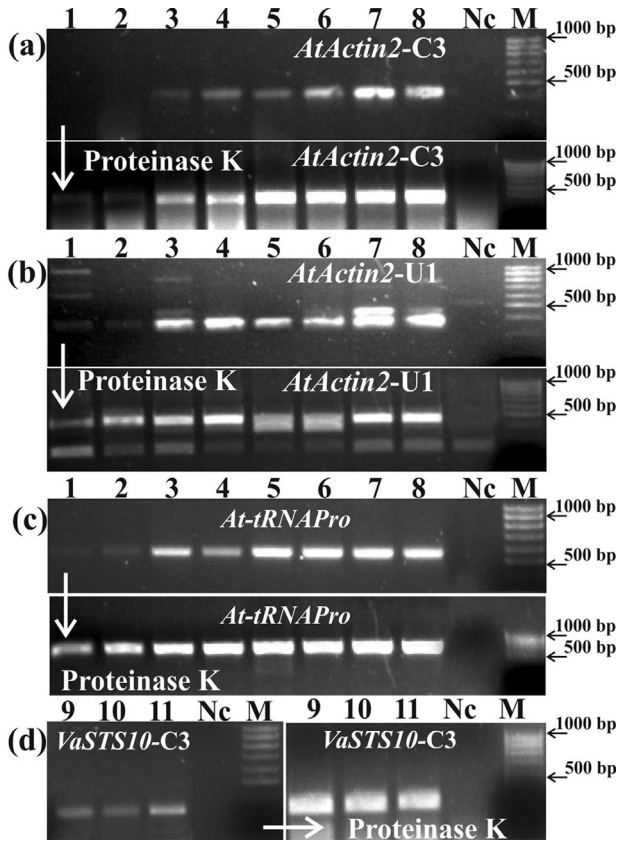

Fig. 8. Electrophoretic separation of PCR products (40 cycles) of the *Actin2* gene of *A. thaliana* (a and b), *At-tRNAPro* DNA of *A. thaliana* (c) and *VaSTS10* gene of *V. amurensis* (d) obtained after additional proteinase K treatment of the extracted DNA. DNA was extracted from the plants collected at different stages of *A. thaliana* life cycle. Two *A. thaliana* plants were collected every 1 (lanes 1 and 2), 4 (lanes 3 and 4), 8 (lanes 5 and 6), and 12 (lanes 7 and 8) weeks after seed sowing. The DNA was extracted from the V2 callus culture of *V. amurensis* cultivated in normal conditions (lane 9) and after treatment with SA at a concentration of 50 μM (lane 10) and 300 μM (lane 11). *AtActin2*-C3 – primers were selected for the end of the *AtActin2* coding sequence (a); *AtActin2*-U1 – primers were selected for 3′ UTR region of the *AtActin2* gene (b); *At-tRNAPro* – primers were selected for the *At-tRNAPro* DNA of *A. thaliana* (c); *VaSTS10*-C3 – primers were selected for the end of *VaSTS10* coding region (d). Lane Nc: negative control (PCR mixture without plant DNA); lane M: synthetic marker.

Application of HotTaq and proteinase K to improve PCR product yield

It is important to find the solution for the problem of low product yield when amplifying highly methylated plant DNA. Diede et al. (2010) report that 5-methylcytosine increases melting temperature T_m of DNA. Bunyan et al. (2011) have shown that DNA methylation status can affect the DNA denaturation rate prior to PCR and markedly decrease PCR efficiency for methylated regions of human DNA. They successfully applied a longer DNA denaturation stage prior to polymerase addition to avoid the observed allele-specific PCR amplification of unmethylated over methylated human DNA. Application of a longer DNA denaturation time (first stage of PCR) for *VaSTS10-C3*, *AtActin2-C3*, *AtActin-U1*, and *At-tRNAPro* regions did not result in a better PCR product yield in our case (data not shown). However, when we applied both a longer DNA denaturation time (95 °C for 10 min for the first stage of PCR) and the HotTag polymerase to amplify DNA, the amounts of PCR products of the *VaSTS10*-C3, *AtActin2*-C3, *AtActin2*-U1, and *At-tRNAPro* considerably increased (Fig. 7a–d).

It is known that methylated DNA may be bound by a variety of DNA-binding proteins, including histones, transcription factors, various polymerases, and nucleases. DNA-binding proteins can recruit additional proteins to the locus, such as histone deacetylases or other chromatin remodeling proteins. We proposed that the highly methylated plant DNA in our probes is likely to be bound by different proteins, which have not been completely removed during DNA purification, and, therefore, access of the Taq DNA polymerase to the methylated sites might be complicated. We hypothesized that using proteinase K for DNA treatment prior to PCR could improve effectiveness of DNA amplification of the *VaSTS10*-C3, *AtActin2*-C3, *AtActin2*-U1, and *At-tRNAPro* regions. As shown in Fig. 8, DNA treatment with proteinase K increased the yield of PCR products of the *VaSTS10*, *AtActin2*-C3, *AtActin2*-U1, and *At-tRNAPro* regions.

After analyzing the cytosine methylation at the CHH, CG, and CHG sites (Tables 1 and 2), we found that weakly amplified DNA regions possessed higher CHH methylation than that of actively amplified DNA regions. The occurrence of CHH sites in the analyzed DNA is generally higher than that of CG and CHG sites. Thus, CHH methylation has a higher impact on PCR efficiency compared to that of CG and CHG methylation due to its higher frequency. Probably, DNA-binding proteins are more essential for the effectiveness of PCR amplification of highly methylated DNA than its denaturation temperature, but this issue demands separate attention.

Conclusion

Taken together, the obtained results suggest that efficient PCR of highly methylated plant DNA can be hampered due to increased DNA denaturation temperatures of methylated DNA and contamination of the DNA samples with DNA-binding proteins. It appears that only the first amplification cycles might be affected by DNA methylation directly or indirectly. However, the efficiency of the first cycle will affect the efficiency of following cycles until saturation. Therefore, this fact does not contradict with conclusions of this study. Further studies are needed to define the main factor decreasing the efficiency of amplification of methylated DNA over DNA methylated at a lower level.

We show that using proteinase K or HotTaq DNA polymerase can alleviate generation of desired amounts of PCR products. The data indicate that for an efficient DNA amplification in PCRs, e.g. for the following DNA sequencing or DNA methylation analysis, it is better to design primers to slightly methylated or completely unmenthylated DNA sequences, which are often at the central gene regions (Lister et al., 2008; Kiselev et al., 2013b; Tyunin et al., 2013). We suggest that using HotTag polymerase or additional procedures (treatment by proteinase K) during DNA extraction is necessary, when it is not possible to design primers to the regions with low methylation levels. DNA treatment with proteinase K prior to PCRs or using HotTaq DNA polymerase can considerably increase PCR product yield and prevent bias when analyzing presence of certain genomic sequences in plant DNA.

To the best of our knowledge, there is only one report on the negative effect of DNA methylation on DNA amplification during PCR (Bunyan et al., 2011). Multiple protocols of plant DNA extraction or commercial DNA extraction kits do not involve treatment with proteinase K (e.g. in Edwards et al., 1991; Echt et al., 1992; Bekesiova et al., 1999; Li et al., 2010; Ahmed et al., 2009; Amani et al., 2011). Since DNA methylation is very common in plant genomes (Finnegan et al., 1998; Vanyushin and Ashapkin, 2011) and a large portion of all cytosines within a plant genome were found to be methylated (Gehring and Henikoff, 2007; Zhang et al., 2010; Capuano et al., 2014), we suggest that proteinase K treatment should be considered as a mandatory step of DNA purification before PCR of those regions, whose methylation status is not known, in order to prevent false-negative results.

Acknowledgements

We thank Dr. Gontcharov A.A. (Institute of Biology and Soil Science, Far East Branch of Russian Academy of Sciences) for useful consultations. This work was supported by grants from the following institutions and foundations: The Russian Foundation for Basic Research (13-04-01902_a) and the Far East Division of the Russian Academy of Sciences.

Appendix A. Supplementary data

Supplementary data associated with this article can be found, in the online version, at http://dx.doi.org/10.1016/j.jplph.2014.10.017.

References

Ahmed I, Islam M, Arshad W, Mannan A, Ahmad W, Mirza B. High-quality plant DNA extraction for PCR: an easy approach. J Appl Genet 2009;50:105–7.
Altschul SF, Gish W, Miller W, Myers EW, Lipman DJ. Basic local alignment search tool. J Mol Biol 1990;215:403–10.
Amani J, Kazemi R, Abbasi AR, Salmanian AH. A simple and rapid leaf genomic DNA extraction method for polymerase chain reaction analysis. Iran J Biotechnol 2011;9:69–71.
Bekesiova I, Nap JP, Mlynarova L. Isolation of high quality DNA and RNA from leaves of the carnivorous plant *Drosera rotundifolia*. Plant Mol Biol Rep 1999;17:269–77.
Boyko A, Kovalchuk I. Epigenetic control of plant stress response. Environ Mol Mutagen 2008;49:61–72.
Bunyan DJ, Bullman HMS, Lever M, Saminathan SD, Keng WT, Araffin R, et al. Different denaturation rates between methylated and non-methylated genomic DNA can result in allele-specific PCR amplification. Open J Genet 2011;1:13–4.
Capuano F, Mülleder M, Kok R, Blom HJ, Ralser M. Cytosine DNA methylation is found in *Drosophila melanogaster* but absent in *Saccharomyces cerevisiae*, *Schizosaccharomyces pombe*, and other yeast species. Anal Chem 2014., http://dx.doi.org/10.1021/ac500447w.
Diede SJ, Guenthoer J, Geng LN, Mahoney SE, Marotta M, Olson JM, et al. DNA methylation of developmental genes in pediatric medulloblastomas identified by denaturation analysis of methylation differences. Proc Natl Acad Sci U S A 2010;107:234–9.
Dubrovina AS, Kiselev KV, Khristenko VS. Expression of calcium-dependent protein kinase (CDPK) genes under abiotic stress conditions in wild-growing grapevine *Vitis amurensis*. J Plant Physiol 2013;170:1491–500.
Echt CS, Erdahl LA, McCoy TJ. Genetic segregation of random amplified polymorphic DNA in diploid cultivated alfalfa. Genome 1992;35:84–7.
Edwards K, Johnstone C, Thompson C. A simple and rapid method for the preparation of plant genomic DNA for PCR analysis. Nucleic Acids Res 1991;19:1349.
Finnegan EJ, Genger RK, Peacock WJ, Dennis ES. DNA methylation in plants. Ann Rev Plant Physiol Plant Mol Biol 1998;49:223–47.
Gehring M, Henikoff S. DNA methylation dynamics in plant genomes. Biochim Biophys Acta 2007;1769:276–86.
Kiselev KV, Dubrovina AS, Veselova MV, Bulgakov VP, Fedoreyev SA, Zhuravlev YN. The *rolB* gene-induced overproduction of resveratrol in *Vitis amurensis* transformed cells. J Biotechnol 2007;128:681–92.
Kiselev KV, Dubrovina AS, Isaeva GA, Zhuravlev YN. The effect of salicylic acid on phenylalanine ammonia-lyase and stilbene synthase gene expression in *Vitis amurensis* cell culture. Russ J Plant Physiol 2010;57:415–21.
Kiselev KV, Shumakova OA, Tchernoded GK. Mutation of *Panax ginseng* genes during long-term cultivation of ginseng cell cultures. J Plant Physiol 2011;168:1280–5.
Kiselev KV, Shumakova OA, Manyakhin AY, Mazeika AN. Influence of calcium influx induced by the calcium ionophore A23187, on resveratrol content and the expression of CDPK and STS genes in the cell cultures of *Vitis amurensis*. Plant Growth Regul 2012;68:371–81.
Kiselev KV, Tyunin AP, Karetin YA. Influence of 5-azacytidine and salicylic acid on demethylase gene expression in cell cultures of *Vitis amurensis* Rupr. Acta Physiol Plant 2013a;35:1843–51.
Kiselev KV, Tyunin AP, Zhuravlev YN. Involvement of DNA methylation in the regulation of *STS10* gene expression in *Vitis amurensis*. Planta 2013b;237:933–41.
Kiselev KV, Tyunin AP, Karetin YA. Salicylic acid induces alterations in the methylation pattern of the *VaSTS1*, *VaSTS2*, and *VaSTS10* genes in *Vitis amurensis* Rupr. cell cultures. Plant Cell Rep 2014., http://dx.doi.org/10.1007/s00299-014-1708-2.
Li JF, Li L, Sheen J. Protocol: a rapid and economical procedure for purification of plasmid or plant DNA with diverse applications in plant biology. Plant Methods 2010;6:1.
Lister R, O'Malley RC, Tonti-Filippini J, Gregory BD, Berry CC, Millar AH, et al. Highly integrated singlebase resolution maps of the epigenome in *Arabidopsis*. Cell 2008;3:523–36.
Okamoto H, Hirochika H. Silencing of transposable elements in plants. Trends Plant Sci 2001;6:527–34.
Rand KN, Mitchell SM, Clark SJ, Molloy PL. Bisulphite differential denaturation PCR for analysis of DNA methylation. Epigenetics 2006;1:94–100.
Severin PM, Zou X, Gaub HE, Schulten K. Cytosine methylation alters DNA mechanical properties. Nucleic Acids Res 2011;39:8740–51.
Tyunin AP, Kiselev KV, Karetin YA. Differences in the methylation patterns of the VaSTS1 and VaSTS10 genes of *Vitis amurensis* Rupr. Biotechnol Lett 2013;35:1525–32.
Vanyushin BF, Ashapkin VV. DNA methylation in higher plants: past, present and future. Biochim Biophys Acta – Gene Regul Mech 2011;1809:360–8.
Zhang M, Kimatu JN, Xu K, Liu B. DNA cytosine methylation in plant development. J Genet Genomics 2010;37:1–12.